



Effect of air annealing on the structural, electrical, and optical properties of V-doped β -Ga₂O₃ single crystals



Pengkun Li^{a,b}, Xueli Han^{a,b}, Duanyang Chen^{a,*}, Qinglin Sai^a, Hongji Qi^{a,c,**}

^a Key Laboratory of Materials for High Power Laser, Shanghai Institute of Optics and Fine Mechanics, Chinese Academy of Sciences, Shanghai 201800, China

^b Center of Materials Science and Optoelectronics Engineering, University of Chinese Academy of Sciences, Beijing 100049, China

^c Hangzhou Institute of Optics and Fine Mechanics, Chinese Academy of Sciences, Hangzhou 311421, China

ARTICLE INFO

Article history:

Received 13 January 2022

Received in revised form 27 February 2022

Accepted 12 March 2022

Available online 15 March 2022

Keywords:

β -Ga₂O₃

V-doped

Annealing

Electrical properties

Optical properties

ABSTRACT

V impurities were intentionally introduced into β -Ga₂O₃ crystals as n-type dopants to improve the n-type conductivity of single-crystal substrates. A high-quality 0.20 mol% V-doped β -Ga₂O₃ single crystal was fabricated, and the effects of air annealing on the structure and the electrical and optical performances of V-doped β -Ga₂O₃ single crystals were systematically studied. The V-doped β -Ga₂O₃ crystal exhibited a high crystal quality, smooth surface, and high carrier concentration. In comparison, the crystalline quality of β -Ga₂O₃ was improved, and it showed a flat surface after the annealing treatment. Compared with that before annealing, the carrier concentration decreased from 5.90×10^{18} to 9.51×10^{17} cm⁻³, the optical transmittance increased in the near-infrared region, and the peak intensity of the A_g⁽³⁾, mid-frequency A_g⁽⁸⁾, A_g⁽⁹⁾, and A_g⁽¹⁰⁾ phonons were changed, which were attributed to the electron traps of the gallium vacancy (V_{Ga}) and the two cation vacancies paired with one cation interstitial atom (2V_{Ga}¹-Ga_i) complex. After annealing, the oxygen vacancy (V_O) was compensated, and the Ga³⁺ content decreased, which were related to the decrease in the free electron concentration. The variations in the V_O and V_{Ga} concentrations resulted in a decrease in the blue luminescence peak area ratio and the formation of a green luminescence peak, respectively. These results can facilitate a better comprehension of the structural and property changes in V-doped β -Ga₂O₃ crystals owing to air annealing.

© 2022 Elsevier B.V. All rights reserved.

1. Introduction

Semiconductor materials have important applications in household appliances, telecommunications, industrial manufacturing, aerospace, and other fields [1–8]. As an emerging semiconductor material, beta-gallium oxide (β -Ga₂O₃) has attracted significant attention owing to its wide band gap ($E_g \approx 4.9$ eV) and high estimated critical electric field ($E_c \approx 8$ MV/cm) [9,10]. It has broad application prospects in high-power electronics and solar-blind photodetectors [11–14]. Large bulk β -Ga₂O₃ single crystals can be produced using various growth methods, including Czochralski (CZ), vertical Bridgman (VB), edge-defined film-fed (EFG), and floating-zone (FZ) growth techniques [15–19]. Among them, the FZ method is widely

used for the preparation of high-quality intrinsic or doped β -Ga₂O₃ single crystals owing to its low cost, short growth cycle.

An important method to improve the performance of crystal optical, electronic, and optoelectronic devices is the tuning of the band gap and carrier concentration of β -Ga₂O₃ crystals by doping with different elements such as Si, Sn, Ta, Nb, and Fe [20–25]. Among them, doping with Si and Sn (4+) are the most common. Theoretically, doping elements with more valence electrons than Si and Sn can produce more free electrons and further improve the conductivity of the β -Ga₂O₃. The ionic radius of V (0.059 nm) with five valence electrons is closer to that of Ga³⁺ than those of Si and Sn; thus, V is an appropriate dopant. Li et al. [26] calculated the β -Ga₂O₃ doped by transition metals (TM) (Sc, Ti, V, Cr, Mn, Fe, Co, Ni, Cu, and Zn) and found that some bandgaps varied regularly with the atomic number, and TM doping makes β -Ga₂O₃ red-shift. V-doped β -Ga₂O₃ films were first prepared by Huang et al. [27]. Nevertheless, at present, there are no reports on the growth of bulk V-doped β -Ga₂O₃ single crystals.

In addition, annealing has a significant effect on the structural and properties of oxide semiconductor materials [28–30]. N.T.Son

* Corresponding author.

** Corresponding author at: Key Laboratory of Materials for High Power Laser, Shanghai Institute of Optics and Fine Mechanics, Chinese Academy of Sciences, Shanghai 201800, China.

E-mail addresses: chenduan yang@siom.ac.cn (D. Chen), qhj@siom.ac.cn (H. Qi).

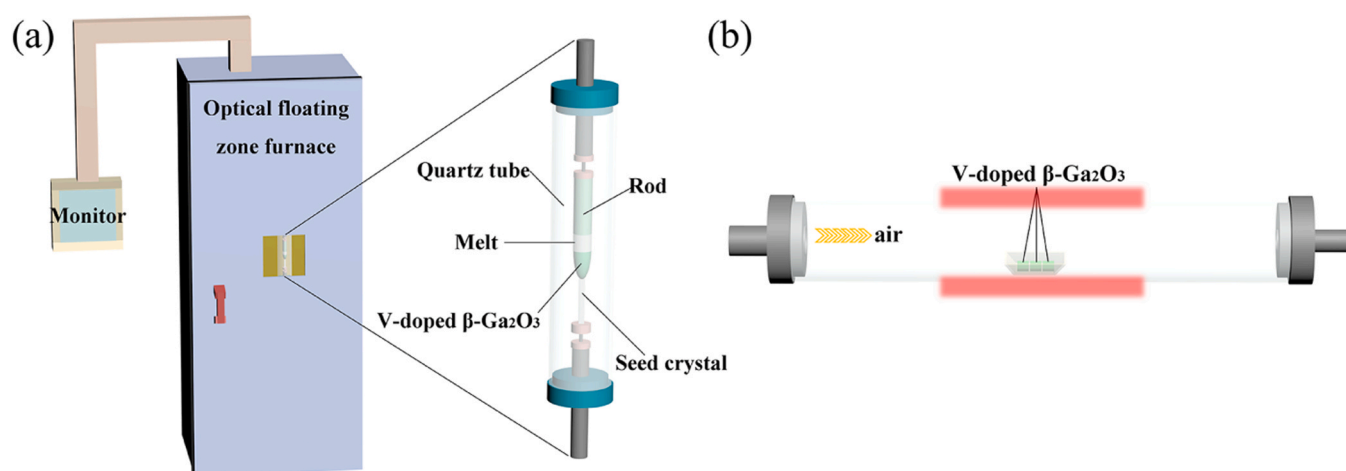


Fig. 1. (a) OFZ apparatus for the growth of β -Ga₂O₃ bulk single crystal. (b) Schematic of the tubular furnace for β -Ga₂O₃ single crystal annealing.

reported that the free carriers of β -Ga₂O₃ can be activated annealing at 1100° for 20 min in nitrogen [31]. A. Luchechko reported the processes of point defects and their associates in β -Ga₂O₃ single crystals (UID, Cr³⁺, and Cr-Mg) annealed at 1300° for 100 h in oxygen or argon [32–34]. The post-annealing changes in the microstructure (such as point defects) of crystals, contributing to the changes in macroscopic physical properties, have remained an important field of research [29–35]. Therefore, it is necessary to study V-doped β -Ga₂O₃ crystals and the effect of the annealing process on their properties.

In this study, a convenient optical floating zone (OFZ) technique was employed to grow V-doped β -Ga₂O₃ single crystals. Then, an air-annealed V-doped β -Ga₂O₃ crystal was obtained by annealing in a tubular furnace. The structure, surface morphology, preferred V⁵⁺ ion sites, Ga/O atomic ratio, and electronic and optical properties of the V-doped β -Ga₂O₃ crystals before and after annealing were systematically investigated using high-resolution X-ray diffraction (HR-XRD), atomic force microscopy (AFM), Raman spectroscopy, X-ray photoelectron spectroscopy (XPS), and Hall, optical transmission, and photoluminescence techniques. The experimental results obtained in this study demonstrate that the crystal properties change owing to the generation of gallium vacancy (V_{Ga}) and complexes of V_{Ga} and the compensation of oxygen vacancy (V_O). These results can promote a better understanding of the structure and the electrical and optical properties of V-doped β -Ga₂O₃ crystals modified by air annealing.

2. Experimental

2.1. Preparation of single crystals

Undoped and 0.20 mol% V-doped β -Ga₂O₃ bulk single crystals were grown by the OFZ method, as shown in Fig. 1(a). High-purity powders of Ga₂O₃ (99.9999%) and V₂O₅ (99.99%) were used as starting materials. Powder mixtures were weighed precisely in stoichiometric proportions, and the Ga₂O₃ (99.9999%) powder was pressed into rods and sintered in air at 1450 °C for 20 h. Single crystals with [010]-orientation were used as seeds, and dry air was used as the growth atmosphere. The β -Ga₂O₃ single crystals were grown at a pull-down rate of 5 mm/h using the reverse rotation of the rods and seeds. The crystal dimensions were 6 mm × 6 mm with the (100) plane. Some of grown crystals were then annealed in a tubular furnace at 1000 °C for 20 h in air atmosphere, as shown in Fig. 1(b). Two crystal forms were used in this study: as-grown and annealed samples.

2.2. Characterization

HR-XRD patterns (in the range of 20–110°) and XRD rocking curves were obtained using a diffractometer (D8 ADVANCE, Bruker Corporation, USA) with an operating voltage of 40 kV and a current of 40 mA (Cu K α line, $\lambda = 1.5406 \text{ \AA}$). The surface morphologies and roughness of the as-prepared samples were characterized using AFM (CSPM 5500, Karaltay (Beijing) Instruments Co., Ltd., China). Raman scattering spectroscopy was performed at room temperature using a spectrometer (iHR550, HORIBA, Ltd., Japan) with a 633 nm laser beam as the excitation source. For the XPS characterization, an ESCALAB 250Xi system (Thermo Fisher Scientific Inc., USA) was used. Hall tests were performed using the Van der Pauw method at room temperature (8404 Hall effect measurement system, Lake Shore Cryotronics, Inc., USA). The in-line optical transmittance spectra of the single crystals were obtained using an ultraviolet/visible/near infrared (UV/VIS/NIR) spectrometer (Lambda 1050+, PerkinElmer Inc., USA) in the scanning range of 200–2000 nm. The room-temperature photoluminescence (RT-PL) spectra were collected using a fluorescence spectrometer (FLS1000, Edinburgh Instruments Ltd., UK) equipped with a continuous wave Xe lamp (266 nm) as the excitation source.

3. Results and discussion

3.1. Structural characterization

The entire body of the 0.20 mol% V-doped β -Ga₂O₃ single crystal was emerald green (as shown in the inset of Fig. 2), suggesting that the overall doping amount of V was relatively uniform. The overall length of the transparent β -Ga₂O₃ crystal without cracks was approximately 45 mm, and its diameter was approximately 6 mm.

Fig. 2 shows the measured HR-XRD patterns for the undoped and 0.20 mol% V-doped β -Ga₂O₃ crystals. Compared with the JCPDF#41–1103 standard card of β -Ga₂O₃, all the sharp diffraction peaks can be indexed to the β phase with the C2/m space group of the monoclinic system. No further impurity phases were detected, indicating the successful synthesis of the undoped and 0.20 mol% V-doped β -Ga₂O₃ single crystals. Each crystal had four strong and sharp diffraction peaks corresponding to the (400), (600), (800), and (1200) planes. After the annealing treatment, the intensity of the diffraction peaks in the measured XRD pattern was noticeably enhanced, indicating a significant improvement in the crystal crystallization quality.

All diffraction peaks shifted slightly to higher Bragg angles after doping with V, suggesting that the interplanar spacing decreased;

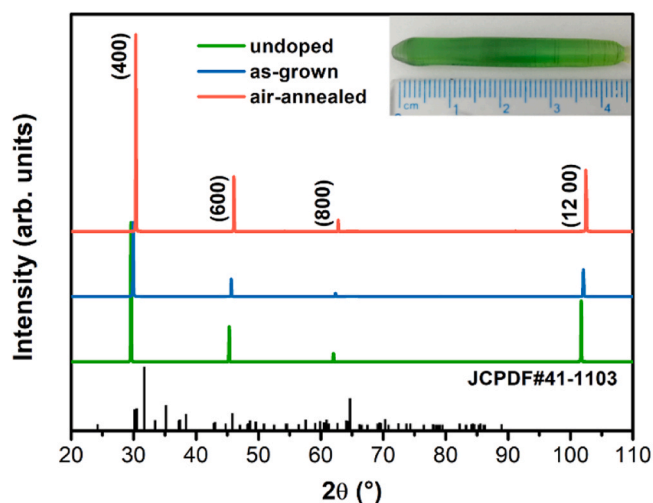


Fig. 2. HR-XRD patterns of the undoped and 0.20 mol% V-doped β -Ga₂O₃ as-grown and air-annealed single crystals. The inset shows an image the 0.20 mol% V-doped β -Ga₂O₃ single crystal.

Table 1

Unit cell parameters of the undoped and V-doped β -Ga₂O₃ as-grown and air-annealed single crystals.

Unit cell parameters	a (Å)	b (Å)	c (Å)	β (°)
Undoped	12.27763	3.05207	5.82802	103.8188
As-grown	12.27216	3.05054	5.82809	103.8186
Air-annealed	12.26851	3.05004	5.82771	103.8172

thus, the lattice constants and unit cell volume decreased. The unit cell parameters of the β -Ga₂O₃ single crystals are listed in Table 1. This can be attributed to the partial replacement of Ga³⁺ (0.062 nm) by V⁵⁺ (0.059 nm), which has a smaller ionic radius. After air annealing at 1000 °C for 20 h, the diffraction peaks of the 0.20 mol% V-doped β -Ga₂O₃ single crystal were further shifted to the higher Bragg angle values, which might be due to the generation of partial V_{Ga} in the crystal, resulting in unit cell shrinkage and narrower lattice plane distance.

3.2. Crystal quality

It is generally accepted that the symmetry of the XRD rocking curve peak is directly related to the structural uniformity of the crystal. The symmetry of the peak pattern indicates that the composition and structure of the crystal are relatively uniform in the diffraction area, and there is no sub grain boundary. To intuitively understand the changes in the quality of the 0.20 mol% V-doped β -Ga₂O₃ crystal before and after annealing, XRD rocking curves were obtained on the (400) diffraction planes, as shown in Fig. 3. The symmetrical and sharp rocking curve diffraction peaks demonstrated that the V-doped β -Ga₂O₃ single crystals had high crystallization quality and the V elements were relatively evenly distributed in the crystals before and after annealing. In addition, the rocking curve of the air-annealed β -Ga₂O₃ single crystal had a higher intensity and a lower full-width at half-maximum (FWHM) value of 64.8°, indicating a better crystal quality, which was attributed to the annealing, which reduced the dislocation density and released the residual stress within the crystal.

The two- (2D) and three-dimensional (3D) AFM images of the as-grown and air-annealed V-doped β -Ga₂O₃ crystals are shown in Fig. 4; the size of the photographs is 5 μ m \times 5 μ m. The surface morphologies of the polished crystals can clearly be observed. The surface of the annealed crystal (Fig. 4(c) and 4(d)) was smoother than that of the grown crystal (Fig. 4(a) and (b)), and the root-mean-

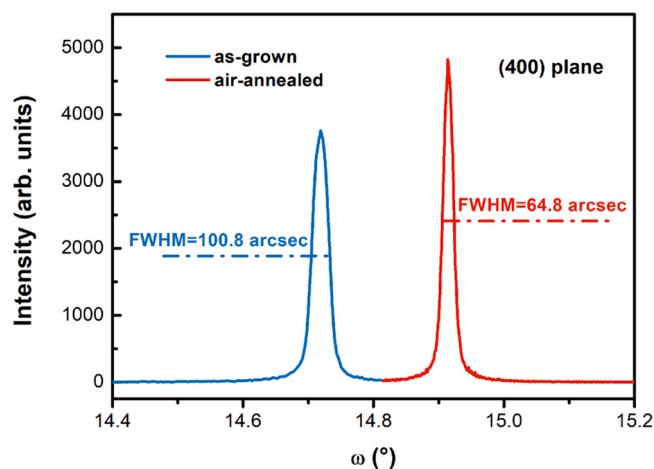


Fig. 3. Rocking curves of the (400)-faced as-grown and air-annealed 0.20 mol% V-doped β -Ga₂O₃ crystals.

square (RMS) roughness was 0.278 nm for the as-grown crystal and 0.138 nm for the air-annealed crystal, indicating that the air-annealed V-doped β -Ga₂O₃ single crystal had an ultra-smooth surface. This characterization result confirms that the crystals have an appropriate quality and smooth surface, which are crucial for high-performance devices.

3.3. Hall characterization

The electrical properties of the as-grown and air-annealed V-doped β -Ga₂O₃ crystals are presented in Table 2. An Ohmic contact was obtained by sputtering 10 nm Ti/ 100 nm Al layers on the four corner surfaces of the samples. The carrier concentration of the undoped sample was $4.84 \times 10^{16} \text{ cm}^{-3}$, with value similar to previous reports [21,36], owing to the presence of shallow-level donors such as Si in the raw material. After doping, the carrier concentration increased to $5.90 \times 10^{18} \text{ cm}^{-3}$, confirming that V provided electrons in the β -Ga₂O₃ crystal and improved the concentration of the effective free carriers. Nevertheless, after annealing, the carrier concentration decreased to $9.51 \times 10^{17} \text{ cm}^{-3}$ compared with that of the as-grown V-doped β -Ga₂O₃, demonstrating that the contribution from the effective free electrons partially disappeared. Furthermore, the mobility and resistivity exhibited an upward trend after annealing in air.

The decrease in the free electron concentration for the annealed sample can be attributed to the increase in the concentration of V_{Ga} and the complexes related to V_{Ga} (2V_{Ga}¹-Ga_i) during annealing in air, because V_{Ga} and complexes of V_{Ga} have low formation energies under oxygen-rich conditions [37,38]. As deep acceptor, V_{Ga} and complexes of V_{Ga} could compensate for the shallow donor. Consequently, the increase in the concentration of V_{Ga} and complexes of V_{Ga} resulted in the decrease in the free carrier concentration. Although the carrier concentration of the air-annealed crystal was significantly lower than that of the as-grown crystal, the carrier mobility increased owing to the decrease in the base number of free electrons. This resulted in a decrease in their collision probability and thus increased the mobility and drift velocity [21,39].

3.4. Raman spectroscopy

The room-temperature Raman scattering spectra of the single-crystal β -Ga₂O₃ is shown in Fig. 5. In the C2/m monoclinic β -Ga₂O₃ structure, 30 phonon modes are generated, of which 27 are optical modes. Among the 27 phonon modes at the Γ -point, 15 phonon modes are Raman active [40]. In the range of 100–1000 cm^{-1} in the

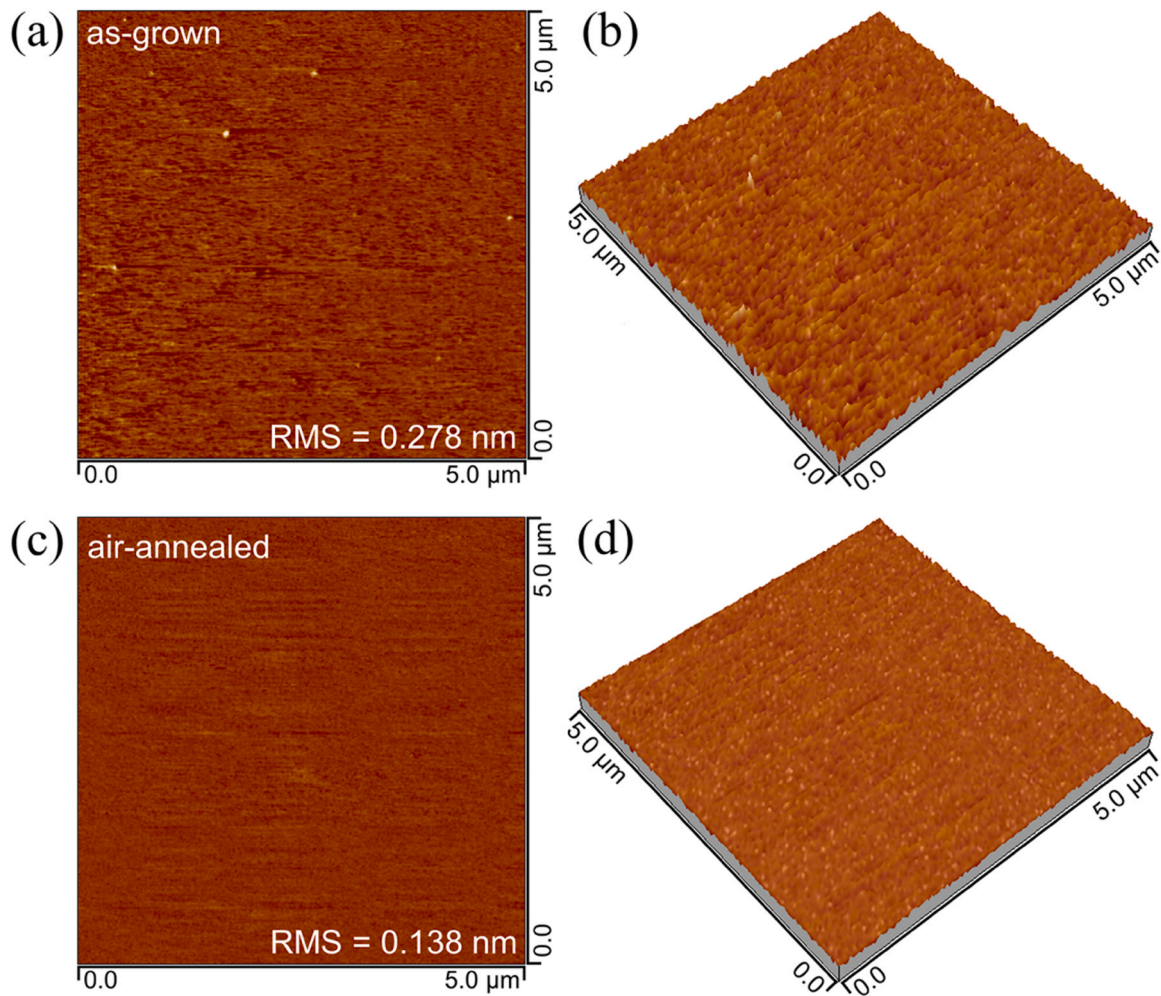


Fig. 4. 2D and 3D AFM surface morphologies of 0.20 mol% V-doped β -Ga₂O₃ single crystals: (a) and (b) as-grown; and (c) and (d) air-annealed.

confocal Raman spectra, 10 Raman phonon peaks were observed, belonging to $B_g^{(2)}$ (144 cm⁻¹), $A_g^{(2)}$ (169 cm⁻¹), $A_g^{(3)}$ (199 cm⁻¹), $A_g^{(4)}$ (319 cm⁻¹), $A_g^{(5)}$ (346 cm⁻¹), $A_g^{(6)}$ (416 cm⁻¹), $A_g^{(7)}$ (476 cm⁻¹), $A_g^{(8)}$ (629 cm⁻¹), $A_g^{(9)}$ (658 cm⁻¹), and $A_g^{(10)}$ (766 cm⁻¹), which is in excellent agreement with the reported data [41,42].

These phonon peaks can be divided into three parts, depending on the type of vibration modes: [40,43] (I) the low-frequency phonon modes (below 250 cm⁻¹, $B_g^{(2)}$, $A_g^{(2)}$, and $A_g^{(3)}$) are attributed to the oscillations and translation motions of tetrahedron-octahedron chains; (II) the mid-frequency modes (250–500 cm⁻¹, $A_g^{(4)}$, $A_g^{(5)}$, $A_g^{(6)}$, and $A_g^{(7)}$) are related to the deformation of the [Ga_{II}O₆] octahedra; and (III) the high-frequency phonon modes (above 500 cm⁻¹, $A_g^{(8)}$, $A_g^{(9)}$, and $A_g^{(10)}$) originate from the stretching and bending of the [Ga_IO₄] tetrahedra.

The intensity of the mid-frequency phonon peak decreased after the addition of V, indicating that the Ga sites in the octahedron (inside the blue rectangle in Fig. 5) were mostly occupied by V ions. The strengths of the $A_g^{(4)}$, $A_g^{(5)}$, $A_g^{(6)}$ and $A_g^{(7)}$ phonon peaks changed

noticeably after annealing, which was attributed to the formation of V_{Ga}^{2+} due to the volatilization of partial V from the octahedron (inside the red rectangle in Fig. 5). As shown by density functional theory (DFT) calculations, cationic vacancies have a low formation energy in an oxygen-rich environment, and tetrahedral V_{Ga}^I is the most favorable [44–46]. Consequently, the concentration of V_{Ga}^I increased during annealing in air atmosphere. The Ga atom in the adjacent tetrahedron shifts in position, effectively producing a $2V_{Ga}^I$ -Ga_i complex as a deep acceptor with an energy lower than that of the isolated vacancy [38]. The $A_g^{(10)}$ phonon peak was significantly suppressed, and the $A_g^{(3)}$ phonon peak was clearly enhanced, which was related to the $2V_{Ga}^I$ -Ga_i complex. This is consistent with the Hall data in Section 3.3.

More accurate information on the positions of the Raman peaks was obtained by employing a Lorentz fit equation, as listed in Table 3. The partial replacement of the large Ga³⁺ by V⁵⁺ with a small ionic radius resulted in a shorter bond length. The bond length is inversely proportional to the Raman phonon frequency [29]. Thus,

Table 2

Room-temperature Hall data of the undoped and V-doped β -Ga₂O₃ as-grown and air-annealed single crystals.

	Type	Resistivity (Ω -cm)	Mobility (cm ² / (V·s))	Carrier concentration (cm ⁻³)
Undoped	N	0.773	166.7	4.84×10^{16}
As-grown	N	0.014	75.0	5.90×10^{18}
Air-annealed	N	0.077	85.3	9.51×10^{17}

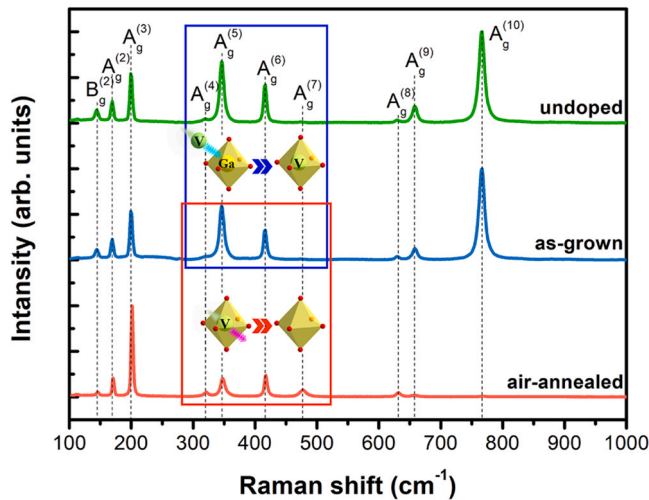


Fig. 5. Raman spectra of the undoped and 0.20 mol% V-doped β -Ga₂O₃ as-grown and air-annealed single crystals.

Table 3
Raman scattering spectra of undoped and V-doped β -Ga₂O₃ single crystals.

Raman mode	Raman shift (cm ⁻¹)		
	Undoped β -Ga ₂ O ₃	0.20 mol% V-doped β -Ga ₂ O ₃	
		As-grown	Air-annealed
B _{(2)g}	143.852	144.134	145.419
A _{(2)g}	169.124	169.151	170.647
A _{(3)g}	199.683	199.733	200.854
A _{(4)g}	318.842	319.575	320.843
A _{(5)g}	346.200	346.244	347.897
A _{(6)g}	416.116	416.122	417.396
A _{(7)g}	476.398	476.635	477.395
A _{(8)g}	629.430	629.590	631.706
A _{(9)g}	658.049	658.280	657.857
A _{(10)g}	766.156	766.272	767.677

the phonon peaks of the 0.20 mol% V-doped single crystal shifted to a higher frequency than that of undoped β -Ga₂O₃. Due to the decrease in material stress, the corresponding Raman peak moves toward a high frequency [47]. The phonon peaks of the air-annealed β -Ga₂O₃ single crystal were further redshifted, suggesting a decrease in the stress and an improvement in the crystal quality. These results are in good agreement with the HR-XRD, rocking curves and AFM results.

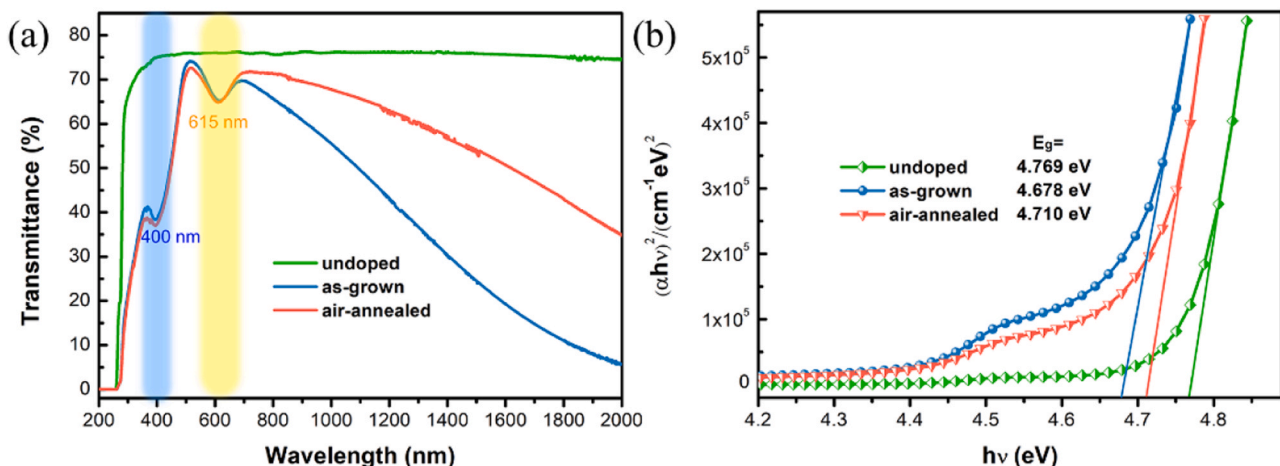


Fig. 6. (a) Optical transmission spectra and (b) absorption edges of the undoped, as-grown, and air-annealed 0.20 mol% V-doped β -Ga₂O₃ crystals.

3.5. Optical transmission spectroscopy

The transmission spectrum is widely used as a characterization method for analyzing the optical band gap and transmittance of a sample. Fig. 6 shows the in-line optical transmission and Tauc plots of the mirror-polished undoped and 0.20 mol% V-doped β -Ga₂O₃ as-grown and air-annealed single crystals. The highest transparency of all crystals was approximately 75%, as shown in Fig. 6(a). The transmittance of crystals in the near-infrared region is closely related to the free carrier concentration. As an n-type dopant, V can provide more free electrons, contributing to the low transmittance of the V-doped β -Ga₂O₃ single crystals in the near-infrared region. V_{Ga} and complexes of V_{Ga} were generated in the V-doped β -Ga₂O₃ crystal during annealing in air [37,38,48], which acted as compensation acceptors, and then captured electrons [38,49], resulting in a decrease in the number of free carriers in the crystal and an increase in the transmittance in the near-infrared region. This is in agreement with the results of Hall characterization.

It should be noted that all V-doped β -Ga₂O₃ as-grown and air-annealed single crystals exhibited two extra absorption peaks around 400 and 615 nm, respectively. These peaks were not observed for the undoped β -Ga₂O₃. Both the crystal color and the two absorption peaks were similar to Cr-doped β -Ga₂O₃ single crystal. Green coloration indicates that there are transitions in the 3d2 configuration [50]. In other words, part of V in V-doped β -Ga₂O₃ may entered the crystal as +3 valence. Huang et al. [27] confirmed the existence of V⁴⁺ and V⁵⁺ ions in V-doped Ga₂O₃ films, and V⁵⁺ ions accounted for a relatively high proportion. Therefore, it is most likely that a large part of V element existed in the form of V⁵⁺ ions, and V³⁺ and V⁴⁺ occupied a minimal fraction in the V-doped β -Ga₂O₃ single crystal. These two broad absorption peaks (400 and 615 nm) can be related to the crystal field splitting electronic transition of V³⁺ and V⁴⁺ in the β -Ga₂O₃ [51]. Furthermore, the two additional absorption peaks were not significantly affected by air annealing. Due to the low proportion of V⁴⁺ and V³⁺, the influence on the above the shift of XRD diffraction peaks and Raman phonon peaks were still dominated by the relatively high V⁵⁺ ions.

Fig. 6(b) shows the optical band gaps of the undoped and 0.20 mol% V-doped β -Ga₂O₃ as-grown and air-annealed single crystals. The band gap of β -Ga₂O₃ decreased from 4.769 eV after V doping, which might be due to the shift of the conduction band to the Fermi level and the significant increase in the state density, resulting in a narrowing of the optical band gap, similar to that of V-doped ZnO [21,52]. After annealing in air, the band gap increased to 4.710 eV, which can be attributed to the absence of V, which maintains the conduction band far from the Fermi level and the reduces

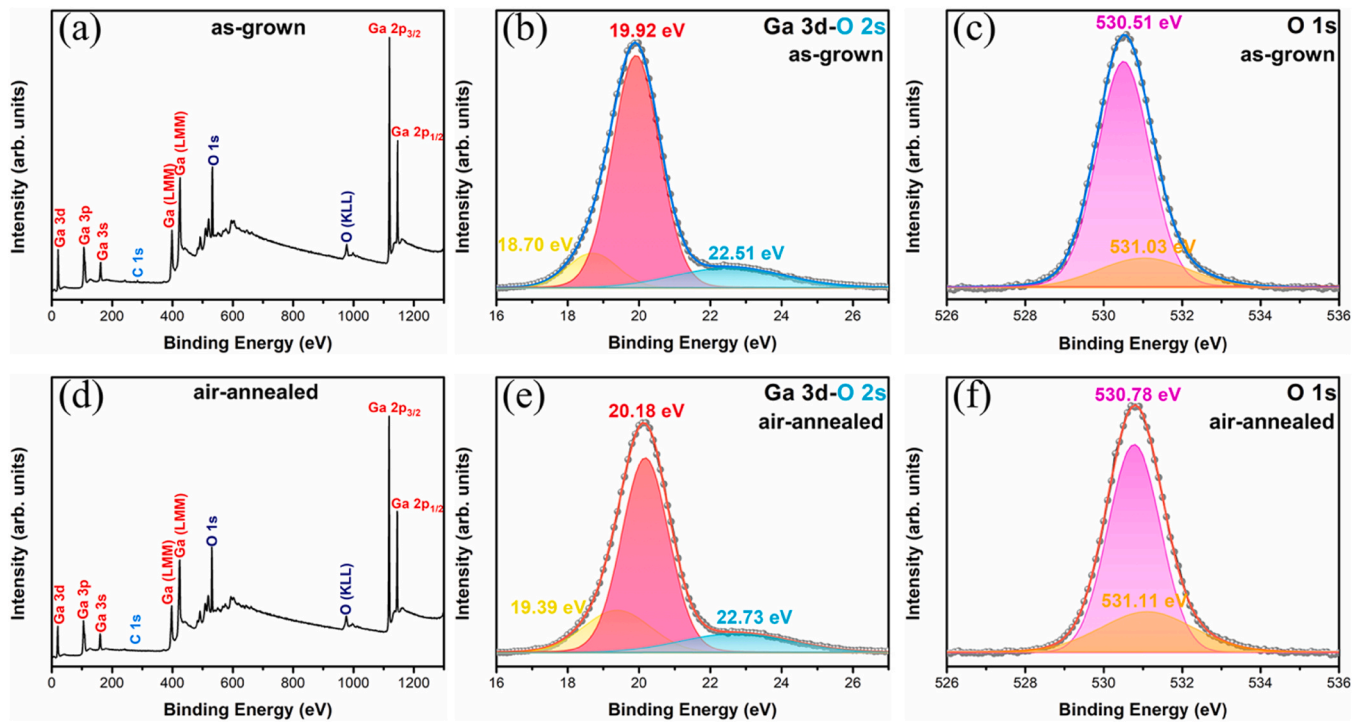


Fig. 7. (a) and (d) Survey XPS spectra of the as-grown and air-annealed 0.20 mol% V-doped β -Ga₂O₃ crystals; high-resolution XPS spectra of (b) and (e) Ga 3d-O 2s; and (c) and (f) O 1s.

the density of states. These results further demonstrate that air annealing partially removes V from the β -Ga₂O₃ crystals.

3.6. XPS analysis

To analyze the constituent elements and relative contents of the samples, XPS was used. To eliminate the experimental error due to the sample surface contamination as much as possible, an Ar ion beam was used to clean the sample surface before the XPS test. Fig. 7(a) and 7(d) show the XPS survey spectra of the as-grown and air-annealed 0.20 mol% V-doped β -Ga₂O₃ samples with Ga, O, and C peaks. Nevertheless, the peak of V could not be observed because the concentration of V was too low to reach the detection limit of the XPS equipment. Fig. 7(b) and 7(c), 7(e) and 7(f) show the high-resolution XPS spectra of the as-grown Ga 3d-O 2s and O 1s and the air-annealed Ga 3d-O 2s and O 1s, respectively. All binding energies were calibrated using the C 1s peak at 284.8 eV.

For the sample before annealing treatment, the Ga 3d and O 1s peaks centered at 19.92 (Ga³⁺) and 530.51 eV (Fig. 7(b)), respectively, belonged to the Ga-O bond of Ga₂O₃. In contrast, the Ga 3d and O 1s peaks shifted to 20.18 (Ga³⁺) and 530.78 eV (Fig. 7(e)), respectively, after annealing in air. The difference in the binding energy of O 1s and Ga 3d before and after annealing is equal to 510.59 and 510.60 eV, respectively. The similarity of these values indicates that the Ga-O bonding before and after annealing is the same [28]. The peaks at 22.51 (Fig. 7(b)) and 22.73 eV (Fig. 7(e)) partially overlapping Ga 3d belonged to O 2s [40,53]. The small peak located at 18.70 eV was defined as Ga¹⁺ (Fig. 7(b)) [28,29]. Nevertheless, after air annealing, the intensity of the small peak with a binding energy of 18.70 eV increased and shifted to 19.39 eV. As the 19.39 eV peak is between the binding energies of Ga¹⁺ and Ga³⁺, it is considered to be corresponding to Ga²⁺ [28,40]. The weakening of the Ga³⁺ peak intensity and the enhancement of the Ga²⁺ peak strength (Fig. 7(e)) suggest that part of Ga³⁺ ions act as electron traps to recapture an electron and obtain Ga²⁺ [28]. This also explains the decrease in the free carrier concentration after annealing.

The main peaks at 530.51 (Fig. 7(c)) and 530.78 eV (Fig. 7(f)) were attributed to Ga₂O₃, which indicates Ga₂O₃ formation [29]. The other peaks located at 531.03 (Fig. 7(c)) and 531.11 eV (Fig. 7(f)) were assigned to the O-Ga bands [28]. The ratio of area of O-Ga after annealing was higher than that before annealing, indicating that the O-Ga bond increased after annealing, which further confirmed the formation of Ga²⁺. The Ga/O ratio of the as-grown and air-annealed V-doped β -Ga₂O₃ was calculated according to the areas of the Ga 3d-O 2s and O 1s XPS core-level peaks and the corresponding sensitivity factors, as shown in Table 4. The Ga/O ratio decreased after annealing, indicating that the O in air entered the lattice and filled part of the V_O [29,44], confirming the repair effect of air annealing on V_O.

3.7. Photoluminescence properties

The room-temperature photoluminescence (RT-PL) spectra of the as-grown and air-annealed 0.20 mol% V-doped β -Ga₂O₃ single crystals were measured, as shown in Fig. 8. Two ultraviolet bands (UV' \approx 3.61 eV and UV \approx 3.31 eV) and one blue band (BB \approx 2.90 eV) were obtained in both PL spectra of the as-growth and air-annealed crystals by Gaussian fitting. In addition, there was an extra broad green band (GB \approx 2.50 eV) in the PL spectrum of the air annealing, which was compared with that of the as-grown V-doped β -Ga₂O₃ single crystal. The ultraviolet emission (UV' and UV) is an inherent property of β -Ga₂O₃ crystals, independent of impurities, and it is attributed to the intrinsic recombination of free electrons with self-trapped holes (STHs) localized on the O_I and O_{II} sites [54,55]. The

Table 4

XPS measurements of the effective areas and Ga/O atomic ratios of the Ga 3d-O 2s, O 1s peaks as-grown and air-annealed 0.20 mol% V-doped β -Ga₂O₃ single crystals.

	Ga 3d	O 1s and O 2s	Ga/O
	Area/SF		
As-grown	69,807	78,511	2:2.25
Air-annealed	55,974	65,245	2:2.33

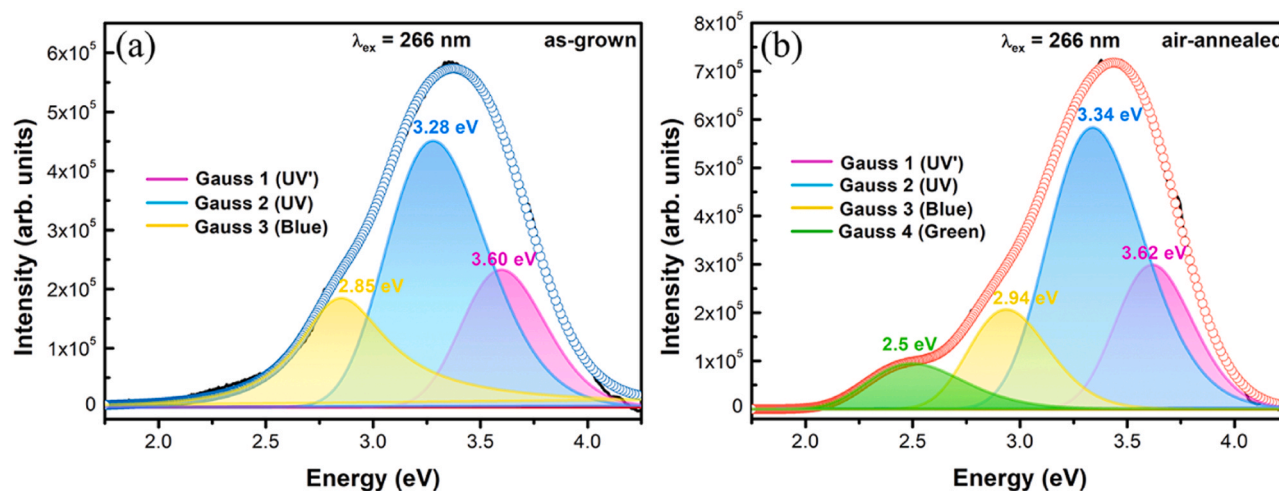


Fig. 8. RT-PL spectra of (a) as-grown, and (b) air-annealed 0.20 mol% V-doped β -Ga₂O₃ single crystals.

Table 5

RT-PL data of 0.20 mol% V-doped β -Ga₂O₃ as-grown and air-annealed single crystals.

	UV' (eV)	Area ratio (%)	UV (eV)	Area ratio (%)	Blue (eV)	Area ratio (%)	Green (eV)	Area ratio (%)
As-grown	3.60 eV	17	3.28 eV	47	2.85 eV	36	—	—
Air-annealed	3.62 eV	18	3.34 eV	49	2.94 eV	19	2.50 eV	14

blue luminescence band is associated with the transition between donor-acceptor pair (DAP) involving deep level donor and acceptor [56]. Possible donors include V_O (ionization energy > 1 eV) and interstitial Ga (Ga_i) [56], while possible acceptors are the V_{Ga} and V_{Ga}-V_O complex [56]. According to the combination of experimental and theoretical calculations, the origin of the ~2.5 eV GB is related to the tetrahedral and octahedral V_{Ga} in crystals [49,57].

The positions and area ratios of the fitted luminescence peaks are listed in Table 5. The total proportion of ultraviolet luminescence bands (UV' and UV) in the spectrum of the air-annealed crystal showed no noticeable change compared to that before annealing. The area ratio of the BB decreased from 36% to 19%, i.e., a decrease by nearly half. The significant change in the BB area ratio is related to the decrease in the V_O concentration by annealing in air atmosphere. V_O was compensated for, and its concentration decreased after annealing, which destroyed the complex structure of the deep acceptors (V_{Ga} and V_{Ga}-V_O complex) and V_O, contributing to a significant attenuation in the proportion of the BB. However, the proportion of GB grew from zero to 14%. This is because the destroyed complex increased the V_{Ga} concentration and resulted in the emergence of the GB. This result is in good agreement with the XPS measurements.

4. Conclusions

In summary, 0.20 mol% V-doped β -Ga₂O₃ single crystals were grown by the OFZ technique. The results pertaining to the XRD rocking curve, Hall effect, Raman spectroscopy, optical transmission, XPS, and PL properties were characterized before and after annealing. The FWHM value of 64.8° confirmed the superior crystalline quality of the crystal after annealing compared to that before annealing. The decrease in the carrier concentration, the increase in transmittance in the near-infrared region, and the change in Raman peak intensity after annealing can be interpreted as the generation of V_{Ga} and the 2V_{Ga}-Ga_i complex as the deep acceptor. Similarly, Ga³⁺ captured electrons and was converted to Ga²⁺, which also resulted in a decrease in the carrier concentration after annealing. The slight increase in the optical band gap after annealing was related to the partial evaporation of V. Furthermore, the proportion of the blue luminescence peak decreased

and an initial green emission peak appeared after annealing in air atmosphere, as measured by RT-PL spectra, which was explained by the decrease in V_O concentration and the increase in V_{Ga} concentration.

CRediT authorship contribution statement

Pengkun Li: Methodology, Formal analysis, Data curation, Software, Investigation, Writing – original draft, Writing – review & editing. **Xueli Han:** Data curation, Software. **Duanyang Chen:** Data curation, Writing – review & editing. **Qinglin Sai:** Formal analysis, Software, Writing – review & editing. **Hongji Qi:** Resources, Supervision, Funding acquisition.

Declaration of Competing Interest

The authors declare that they have no known competing financial interests or personal relationships that could have appeared to influence the work reported in this paper.

Acknowledgments

We would like to thank Hangzhou Fujia Gallium Technology Co., Ltd. for its help in crystal growth, processing and testing. This work was supported by the Shanghai Science and Technology Commission (Grant number: 20511107400).

References

- [1] J. Hong, H. Wen, J. He, J. Liu, Y. Dan, J.W. Tomm, F. Yue, J. Chu, C. Duan, Stimulated emission at 1.54 μ m from erbium/oxygen-doped silicon-based light-emitting diodes, *Photon. Res.* 9 (2021) 714.
- [2] S.R. Kodigala, Surface studies and photoluminescence of GaN epitaxial layers grown by MOCVD technique for applications of solar cells and light emitting devices, *J. Alloy. Compd.* 674 (2016) 435–446.
- [3] F. Hu, S. Chen, G. Li, P. Zou, J. Zhang, J. Hu, J. Zhang, Z. He, S. Yu, F. Jiang, N. Chi, Si-substrate LEDs with multiple superlattice interlayers for beyond 24 Gbps visible light communication, *Photon. Res.* 9 (2021) 1581.
- [4] A. Waseem, M.A. Johar, M.A. Hassan, I.V. Bagal, A. Abdullah, J.-S. Ha, J.K. Lee, S.-W. Ryu, Flexible self-powered piezoelectric pressure sensor based on GaN/p-GaN coaxial nanowires, *J. Alloy. Compd.* 872 (2021) 159661.

- [5] J. Wang, C. Chu, K. Tian, J. Che, H. Shao, Y. Zhang, K. Jiang, Z.-H. Zhang, X. Sun, D. Li, Polarization assisted self-powered GaN-based UV photodetector with high responsivity, *Photon. Res.* 9 (2021) 734–740.
- [6] Z. Dai, Y. Liu, G. Yang, F. Xie, C. Zhu, Y. Gu, N. Lu, Q. Fan, Y. Ding, Y. Li, Y. Yu, X. Zhang, Carrier transport and photoconductive gain mechanisms of AlGaIn MSM photodetectors with high Al Content, *Chin. Opt. Lett.* 19 (2021) 082504.
- [7] Z. Dang, Y. Luo, X.-S. Wang, M. Imran, P. Gao, Electron-beam-induced degradation of halide-perovskite-related semiconductor nanomaterials, *Chin. Opt. Lett.* 19 (2021) 030002.
- [8] L. Duan, H. Zhu, M. Li, X. Zhao, Y. Wang, Y. Zhang, L. Yu, Atom substitution method to construct full-solar-spectrum absorption MoSeS/TiO₂ nanotube arrays for highly efficient hydrogen evolution, *J. Alloy. Compd.* 889 (2021) 161694.
- [9] A. Kuramata, K. Koshi, S. Watanabe, Y. Yamaoka, T. Masui, S. Yamakoshi, High-quality β -Ga₂O₃ single crystals grown by edge-defined film-fed growth, *Jpn. J. Appl. Phys.* 55 (2016) 1202A1202.
- [10] S.J. Pearton, J. Yang, P.H. Cary, F. Ren, J. Kim, M.J. Tadjer, M.A. Mastro, A review of Ga₂O₃ materials, processing, and devices, *Appl. Phys. Rev.* 5 (2018) 011301.
- [11] F. Zhou, H. Gong, W. Xu, X. Yu, Y. Xu, Y. Yang, F.-f Ren, S. Gu, Y. Zheng, R. Zhang, J. Ye, H. Lu, 1.95-kV beveled-mesa NiO/ β -Ga₂O₃ heterojunction diode with 98.5% conversion efficiency and over million-times overvoltage ruggedness, *IEEE T. Power Electr.* 37 (2022) 1223–1227.
- [12] Z. Liu, M. Zhang, L. Yang, S. Li, S. Zhang, K. Li, P. Li, Y. Guo, W. Tang, Enhancement-mode normally-off β -Ga₂O₃:Si metal-semiconductor field-effect deep-ultraviolet phototransistor, *Semicond. Sci. Tech.* 37 (2021) 015001.
- [13] X. Li, J.G. Yang, H.P. Ma, Y.H. Liu, Z.G. Ji, W. Huang, X. Ou, D.W. Zhang, H.L. Lu, Atomic layer deposition of Ga₂O₃/ZnO composite films for high-performance forming-free resistive switching memory, *ACS Appl. Mater. Inter.* 12 (2020) 30538–30547.
- [14] M. Chang, J. Ye, Y. Su, J. Shen, N. Zhao, J. Wang, H. Song, X. Zhong, S. Wang, W. Tang, D. Guo, Zn/Mg co-alloyed for higher photoelectric performance and unchanged spectral response in β -Ga₂O₃ solar-blind photodetector, *J. Phys. D: Appl. Phys.* 55 (2021) 035103.
- [15] Y. Tomm, P. Reiche, D. Klimm, T. Fukuda, Czochralski grown Ga₂O₃ crystals, *J. Cryst. Growth* 220 (2000) 510–514.
- [16] K. Hoshikawa, T. Kobayashi, Y. Matsuki, E. Ohba, T. Kobayashi, 2-inch diameter (1 0 0) β -Ga₂O₃ crystal growth by the vertical Bridgman technique in a resistance heating furnace in ambient air, *J. Cryst. Growth* 545 (2020) 125724.
- [17] H. Aida, K. Nishiguchi, H. Takeda, N. Aota, K. Sunakawa, Y. Yaguchi, Growth of β -Ga₂O₃ single crystals by the edge-defined, film fed growth method, *Jpn. J. Appl. Phys.* 47 (2008) 8506–8509.
- [18] B. Fu, W. Mu, J. Zhang, X. Wang, W. Zhuang, Y. Yin, Z. Jia, X. Tao, A study on the technical improvement and the crystalline quality optimization of columnar β -Ga₂O₃ crystal growth by an EFG method, *CrystEngComm* 22 (2020) 5060–5066.
- [19] E. Villora, K. Shimamura, Y. Yoshikawa, K. Aoki, N. Ichinose, Large-size β -Ga₂O₃ single crystals and wafers, *J. Cryst. Growth* 270 (2004) 420–426.
- [20] J. Zhang, C. Xia, Q. Deng, W. Xu, H. Shi, F. Wu, J. Xu, Growth and characterization of new transparent conductive oxides single crystals β -Ga₂O₃: Sn, *J. Phys. Chem. Solid.* 67 (2006) 1656–1659.
- [21] H. Cui, H.F. Mohamed, C. Xia, Q. Sai, W. Zhou, H. Qi, J. Zhao, J. Si, X. Ji, Tuning electrical conductivity of β -Ga₂O₃ single crystals by Ta doping, *J. Alloy. Compd.* 788 (2019) 925–928.
- [22] T. Oshima, A. Hashiguchi, T. Moribayashi, K. Koshi, K. Sasaki, A. Kuramata, O. Ueda, T. Oishi, M. Kasu, Electrical properties of Schottky barrier diodes fabricated on (001) β -Ga₂O₃ substrates with crystal defects, *Jpn. J. Appl. Phys.* 56 (2017) 086501.
- [23] M. Yamaga, E.G. Villora, K. Shimamura, N. Ichinose, M. Honda, Donor structure and electric transport mechanism in β -Ga₂O₃, *Phys. Rev. B* 68 (2003).
- [24] W. Zhou, C. Xia, Q. Sai, H. Zhang, Controlling n-type conductivity of β -Ga₂O₃ by Nb doping, *Appl. Phys. Lett.* 111 (2017) 242103.
- [25] J. Chen, H. Tang, Z. Li, Z. Zhu, M. Gu, J. Xu, X. Ouyang, B. Liu, Highly sensitive X-ray detector based on a β -Ga₂O₃:Fe single crystal, *Opt. Express* 29 (2021) 23292–23299.
- [26] S. Gao, W. Li, J. Dai, Q. Wang, Z. Suo, Effect of transition metals doping on electronic structure and optical properties of β -Ga₂O₃, *Mater. Res. Express* 8 (2021) 025904.
- [27] J. Huang, Y. Hu, T. Zou, K. Tang, Z. Zhang, Y. Ma, B. Li, L. Wang, Y. Lu, Investigation of properties of transparent and conducting V-doped Ga₂O₃ films, *Surf. Coat. Tech.* 366 (2019) 70–74.
- [28] H. Cui, Q. Sai, H. Qi, J. Zhao, J. Si, M. Pan, Analysis on the electronic trap of β -Ga₂O₃ single crystal, *J. Mater. Sci.* 54 (2019) 12643–12649.
- [29] N. Zhang, H. Liu, Q. Sai, C. Shao, C. Xia, L. Wan, Z.C. Feng, H.F. Mohamed, Structural and electronic characteristics of Fe-doped β -Ga₂O₃ single crystals and the annealing effects, *J. Mater. Sci.* 56 (2021) 13178–13189.
- [30] A. Okada, M. Nakatani, L. Chen, R.A. Ferreyra, K. Kadono, Effect of annealing conditions on the optical properties and surface morphologies of (-201)-oriented β -Ga₂O₃ crystals, *Appl. Surf. Sci.* 574 (2022) 151651.
- [31] N.T. Son, K. Goto, K. Nomura, Q.T. Thieu, R. Togashi, H. Murakami, Y. Kumagai, A. Kuramata, M. Higashiwaki, A. Koukitsu, S. Yamakoshi, B. Monemar, E. Janzén, Electronic properties of the residual donor in unintentionally doped β -Ga₂O₃, *J. Appl. Phys.* 120 (2016) 235703.
- [32] A. Luchechko, V. Vasylytsiv, L. Kostyk, O. Tsvetkova, B. Pavlyk, The effect of Cr³⁺ and Mg²⁺ impurities on thermoluminescence and deep traps in β -Ga₂O₃ crystals, *ECS J. Solid State Sci. Technol.* 9 (2020) 045008.
- [33] A. Luchechko, V. Vasylytsiv, L. Kostyk, O. Tsvetkova, B. Pavlyk, Thermally stimulated luminescence and conductivity of β -Ga₂O₃ crystals, *J. Nano Electron. Phys.* 11 (2019) 03035.
- [34] V. Vasylytsiv, A. Luchechko, Y. Zhydachevskyy, L. Kostyk, R. Lys, D. Slobodzyan, R. Jakiela, B. Pavlyk, A. Suchocki, Correlation between electrical conductivity and luminescence properties in β -Ga₂O₃:Cr³⁺ and β -Ga₂O₃:Cr,Mg single crystals, *J. Vac. Sci. Technol. A* 39 (2021) 033201.
- [35] Z. Shen, W. Xu, Y. Xu, H. Huang, J. Lin, T. You, J. Ye, X. Ou, The effect of oxygen annealing on characteristics of β -Ga₂O₃ solar-blind photodetectors on SiC substrate by ion-cutting process, *J. Alloy. Compd.* 889 (2021) 161743.
- [36] K. Irmscher, Z. Galazka, M. Pietsch, R. Uecker, R. Fornari, Electrical properties of β -Ga₂O₃ single crystals grown by the Czochralski method, *J. Appl. Phys.* 110 (2011) 063720.
- [37] T. Zacherle, P.C. Schmidt, M. Martin, Ab initio calculations on the defect structure of β -Ga₂O₃, *Phys. Rev. B* 87 (2013) 235206.
- [38] J.M. Johnson, Z. Chen, J.B. Varley, C.M. Jackson, E. Farzana, Z. Zhang, A.R. Arehart, H.-L. Huang, A. Genc, S.A. Ringel, C.G. Van de Walle, D.A. Muller, J. Hwang, Unusual formation of point-defect complexes in the ultrawide-band-gap semiconductor β -Ga₂O₃, *Phys. Rev. X* 9 (2019) 041027.
- [39] P. Li, Y. Bu, D. Chen, Q. Sai, H. Qi, Investigation of the crack extending downward along the seed of the β -Ga₂O₃ crystal grown by the EFG method, *CrystEngComm* 23 (2021) 6300–6306.
- [40] B.R. Tak, S. Dewan, A. Goyal, R. Pathak, V. Gupta, A.K. Kapoor, S. Nagarajan, R. Singh, Point defects induced work function modulation of β -Ga₂O₃, *Appl. Surf. Sci.* 465 (2019) 973–978.
- [41] B.M. Janzen, P. Mazzolini, R. Gillen, A. Falkenstein, M. Martin, H. Tornatzky, J. Maultzsch, O. Bierwagen, M.R. Wagner, Isotopic study of Raman active phonon modes in β -Ga₂O₃, *J. Mater. Chem. C* 9 (2021) 2311–2320.
- [42] S. Mandal, K. Arts, H.C.M. Knoops, J.A. Cuenca, G.M. Klemencic, O.A. Williams, Surface zeta potential and diamond growth on gallium oxide single crystal, *Carbon* 181 (2021) 79–86.
- [43] F. Shi, H. Qiao, Influence of hydrothermal reaction time on crystal qualities and photoluminescence properties of β -Ga₂O₃ nanorods, *J. Mater. Sci.: Mater. Electron.* 31 (2020) 20223–20231.
- [44] J.B. Varley, J.R. Weber, A. Janotti, C.G. Van de Walle, Oxygen vacancies and donor impurities in β -Ga₂O₃, *Appl. Phys. Lett.* 97 (2010) 142106.
- [45] J.B. Varley, H. Peelaers, A. Janotti, C.G. Van de Walle, Hydrogenated cation vacancies in semiconducting oxides, *J. Phys.: Condens. Matter* 23 (2011) 334212.
- [46] M.E. Ingebrigtsen, A.Y. Kuznetsov, B.G. Svensson, G. Alfieri, A. Mihaila, U. Badstübner, A. Perron, L. Vines, J.B. Varley, Impact of proton irradiation on conductivity and deep level defects in β -Ga₂O₃, *APL Mater.* 7 (2019) 022510.
- [47] I.H. Lee, I.H. Choi, C.R. Lee, E.J. Shin, D. Kim, S.K. Noh, S.J. Son, K.Y. Lim, H.J. Lee, Stress relaxation in Si-doped GaN studied by Raman spectroscopy, *J. Appl. Phys.* 83 (1998) 5787–5791.
- [48] H. Tang, N. He, Z. Zhu, M. Gu, B. Liu, J. Xu, M. Xu, L. Chen, J. Liu, X. Ouyang, Temperature-dependence of X-ray excited luminescence of β -Ga₂O₃ single crystals, *Appl. Phys. Lett.* 115 (2019) 071904.
- [49] H. Gao, S. Muralidharan, N. Pronin, M.R. Karim, S.M. White, T. Asel, G. Foster, S. Krishnamoorthy, S. Rajan, L.R. Cao, M. Higashiwaki, H. von Wenckstern, M. Grundmann, H. Zhao, D.C. Look, L.J. Brillson, Optical signatures of deep level defects in Ga₂O₃, *Appl. Phys. Lett.* 112 (2018) 242102.
- [50] A. Luchechko, V. Vasylytsiv, Y. Zhydachevskyy, M. Kushlyk, S. Ubizskii, A. Suchocki, Luminescence spectroscopy of Cr³⁺ ions in bulk single crystalline β -Ga₂O₃, *J. Phys. D.: Appl. Phys.* 53 (2020) 354001.
- [51] V. Janakiraman, V. Tamilnayagam, R.S. Sundararajan, S. Suresh, C.S. Biju, Structural and optical properties of pure SnO₂ and V₂O₅/SnO₂ nanocomposite thin films for gas sensing application, *J. Mater. Sci.: Mater. Electron.* 31 (2020) 15477–15488.
- [52] B. Feng, W. Mao, The mechanism of the effect of V doping on the thermoelectric properties of ZnO ceramics, *J. Solid State Chem.* 305 (2022) 122645.
- [53] A. Navarro-Quezada, S. Alamé, N. Esser, J. Furthmüller, F. Bechstedt, Z. Galazka, D. Skuridina, P. Vogt, Near valence-band electronic properties of semiconducting β -Ga₂O₃ (100) single crystals, *Phys. Rev. B* 92 (2015) 195306.
- [54] T. Harwig, F. Kellendonk, S. Slappendel, The ultraviolet luminescence of β -galliumsesquioxide, *J. Phys. Chem. Solids* 39 (1978) 675–680.
- [55] Y. Wang, P.T. Dickens, J.B. Varley, X. Ni, E. Lotubai, S. Sprawls, F. Liu, V. Lordi, S. Krishnamoorthy, S. Blair, K.G. Lynn, M. Scarpulla, B. Sensale-Rodriguez, Incident wavelength and polarization dependence of spectral shifts in β -Ga₂O₃ UV photoluminescence, *Sci. Rep.* 8 (2018) 18075.
- [56] T. Harwig, F. Kellendonk, Some observations on the photoluminescence of doped β -galliumsesquioxide, *J. Solid State Chem.* 24 (1978) 255–263.
- [57] Q.D. Ho, T. Frauenheim, P. Deák, Origin of photoluminescence in β -Ga₂O₃, *Phys. Rev. B* 97 (2018) 115163.